

## Production of Polyhydroxyalkanoates with High 3-Hydroxydodecanoate Monomer Content by *fadB* and *fadA* Knockout Mutant of *Pseudomonas putida* KT2442

Shao-Ping Ouyang,<sup>†,§</sup> Rong Cong Luo,<sup>‡,§</sup> Si-Si Chen,<sup>†</sup> Qian Liu,<sup>†</sup> Ahleum Chung,<sup>†</sup> Qiong Wu,<sup>†</sup> and Guo-Qiang Chen<sup>\*,†,‡</sup>

Department of Biological Sciences and Biotechnology, Tsinghua University, Beijing 100084, China, and Multidisciplinary Research Center, Shantou University, Shantou 515063, China

Received February 25, 2007; Revised Manuscript Received April 26, 2007

*Pseudomonas putida* KT2442 produces medium-chain-length (MCL) polyhydroxyalkanoates (PHA) consisting of 3-hydroxyhexanoate (HHx), 3-hydroxyoctanoate (HO), 3-hydroxydecanoate (HD), and 3-hydroxydodecanoate (HDD) from a wide-range of carbon sources. In this study, *fadA* and *fadB* genes encoding 3-ketoacyl-CoA thiolase and 3-hydroxyacyl-CoA dehydrogenase in *P. putida* KT2442 were knocked out to weaken the  $\beta$ -oxidation pathway. Two-step culture was proven as the optimal method for PHA production in the mutant termed *P. putida* KTOY06. In a shake-flask culture, when dodecanoate was used as a carbon source, *P. putida* KTOY06 accumulated 84 wt % PHA, much higher than 50 wt % PHA in its wild type KT2442. The PHA monomer composition was completely different: the HDD fraction in PHA produced by KTOY06 was 41 mol %, much higher compared with 7.5 mol % only in KT2442. The fermentor-scale culture indicated the HDD fraction in PHA decreased during the culture time from 35 to 25 mol % in a one-step fermentation process or from 75 to 49 mol % in a two-step fermentation process. It is for the first time that PHA with a dominant HDD fraction was produced. Thermal and mechanical properties assays indicated that this new type PHA with a high HDD fraction had higher crystallinity and tensile strength than PHA with a low HDD fraction did, demonstrating an improved application property.

### Introduction

Polyhydroxyalkanoates (PHA) are biopolymers synthesized by various bacteria from renewable sources.<sup>1–3</sup> PHA have attracted much attention from academic and industrial communities for their unique properties of biodegradability and biocompatibility.<sup>4–6</sup> Medium-chain-length (MCL) PHA consists of monomers of 3-hydroxyhexanoate (HHx), 3-hydroxyoctanoate (HO), 3-hydroxydecanoate (HD), 3-hydroxydodecanoate (HDD), or even higher chain length monomers.<sup>7</sup> The material properties of MCL PHA are completely different from polyhydroxybutyrate (PHB). MCL PHA is amorphous or semicrystalline and viscoelastic and has low  $T_m$ , weaker tensile strength, and longer elongation rate compared with PHB. They can be used as an elastomer or blending materials to improve the physical properties of other PHAs.<sup>8–10</sup>

Many species of *Pseudomonas* have been reported to have the abilities of accumulating MCL PHA from fatty acids or glucose.<sup>7,11–13</sup> When fatty acids were used as the sole carbon sources, the  $\beta$ -oxidation pathway played an important role in providing intermediates for PHA synthesis.<sup>14</sup> Since the  $\beta$ -oxidation pathway has a close relationship with MCL PHA synthesis, many researchers have studied the metabolic engineering of the  $\beta$ -oxidation pathway to increase PHA accumulation.<sup>14–20</sup> 3-Ketoacyl-CoA thiolase (FadA) and 3-hydroxyacyl-CoA dehydrogenase (FadB) are two important enzymes catalyzing the last two steps in the  $\beta$ -oxidation pathway. Snell et al. and Park et al. reported that MCL PHA production could be enhanced in

*fadB* mutant *E. coli* harboring only the *phaC* gene.<sup>14–16</sup> Olivera et al. found that in *Pseudomonas* spp. the mutation of some genes involved in the  $\beta$ -oxidation pathway (*fadA*, *fadB*, or *fadBA*) elicits a strong intracellular accumulation of unusual homo- or copolymers that dramatically alter the morphology of these bacteria, as more than 90% of the cytoplasm is occupied by these macromolecules.<sup>18</sup>

*Pseudomonas putida* KT2442 was a rifampicin-resistant derivative<sup>21</sup> of *P. putida* KT2440, which was a well-known MCL PHA producer.<sup>22–23</sup> The whole genomic DNA of *P. putida* KT2440 was sequenced and released in 2002.<sup>24</sup> KT2442 could accumulate MCL PHA consisting of HHx, HO, HD, and HDD when dodecanoate was used as the carbon source, in which the HDD fraction was less than 15 mol %.<sup>7</sup> Our recent study established a rapid gene knockout method for *P. putida* KT2442.<sup>7</sup> In this study, a  $\beta$ -oxidation-impaired mutant of *P. putida* KT2442 was constructed by deleting *fadB* and *fadA* genes to synthesize PHA with a high HDD fraction over 40 mol %. The effects of gene knockout on PHA accumulation, cell growth, and PHA monomer composition were investigated. The physical properties of MCL PHA with different HDD fraction were also characterized by gel permeation chromatography (GPC), differential scanning calorimetry (DSC), Fourier transform infrared (FTIR), and stress–strain measurement.

### Materials and Methods

**Bacterial Strains.** *E. coli* S17–1 (*recA*; harbors the *tra* genes of plasmid RP4 in the chromosome; *proA*, *thi-1*)<sup>25</sup> was used as the host for plasmid construction and as a vector donor via conjugation. *P. putida* KT2442 was a MCL PHA producer with ampicillin resistance, which was kindly provided by Dr. Bernard Witholt (ETH Zürich, Switzerland). *P. putida* KTOY04, KTOY06 and KTOY08 were gene knockout mutants of *P. putida* KT2442. (Table 1).

\* Author to whom correspondence should be addressed. Phone: +86-754-2901186. Fax: +86-754-2901175. E-mail: chengq@stu.edu.cn.

<sup>†</sup> Tsinghua University.

<sup>‡</sup> Shantou University.

<sup>§</sup> These authors contributed equally to this paper.

**Table 1.** Bacterial Strains and Plasmids Used in This Study

plasmids or strains	relevant characteristics	ref
pK18mobsacB	suicide plasmid for gene knockout, Kam <sup>R</sup>	26
pSPK08	a fragment from KT2442 genome containing partial DNA sequence of <i>fadB2x</i> , whole length of <i>fadAx</i> and its downstream sequence was inserted in pK18mobsacB	this study
pSPK09	pSPK08 completely digested by <i>Sall</i> , and then the large fragment was self-ligated, as a result, only partial length of <i>fadB2x</i> and <i>fadAx</i> were inserted into pK18mobsacB	this study
pSPK10	a fragment from KT2442 genome containing partial DNA sequence of <i>fadB</i> , whole length of <i>fadA</i> and its downstream sequence was inserted in pK18mobsacB	this study
pSPK11	pSPK10 completely digested by <i>Sall</i> , and then the large fragment was self-ligated, as a result, only partial length of <i>fadB</i> and <i>fadA</i> were inserted into pK18mobsacB	this study
<i>E. coli</i> S17-1	<i>recA</i> ; harbors the <i>tra</i> genes of plasmid RP4 in the chromosome; <i>proA</i> , <i>thi-1</i>	25
<i>P. putida</i> KT2442	MCL PHA producer strain; rifampicin and ampicillin resistance;	7
<i>P. putida</i> KTOY04	<i>P. putida</i> KT2442 mutant ( $\Delta fadB2x \Delta fadAx$ )	this study
<i>P. putida</i> KTOY06	<i>P. putida</i> KT2442 mutant ( $\Delta fadB \Delta fadA$ )	this study
<i>P. putida</i> KTOY08	<i>P. putida</i> KT2442 mutant ( $\Delta fadB2x \Delta fadAx \Delta fadB \Delta fadA$ )	this study

**Plasmids Construction.** pK18mobsacB<sup>26</sup> was a suicide vector which was a gift from Dr. Andreas Schäfer of the University of Bielefeld (Bielefeld, Germany). Plasmids pSPK08, pSPK09, pSPK10, and pSPK11 were pK18mobsacB derivatives. A fragment from *P. putida* KT2442 genome containing whole length of *fadB2x fadAx* and partial length of the upstream and downstream DNA were amplified by PCR using the following two primers: 5' primer ATTTCTAGAGCTGAAC-CCGGATGGC and 3' primer AATAAGCTTGCCGAAGCGCAG-GATC. PCR products and pK18mobsacB were double-digested by *XbaI* and *HindIII* and then ligated to form a new plasmid pSPK08. Plasmid pSPK08 was completely digested by *Sall*, and then the large fragment was self-ligated to form pSPK09. As a result, two DNA fragments, containing partial 5' sequence of *fadB2x* and partial 3' sequence of *fadAx*, were inserted into pK18mobsacB in pSPK09. Similarly, a fragment from the *P. putida* KT2442 genome containing a partial length of *fadB* and *fadA* were amplified by PCR using the following two primers: 5' primer ATTTCTAGAGCAGATGATGGCCTTC and 3' primer CTGAAGCTTTGTAATGCCGGTATAC. PCR products and pK18mobsacB were double-digested by *XbaI* and *HindIII* and then ligated together to form a new plasmid pSPK10. Plasmid pSPK10 was completely digested by *Sall*, and then the large fragment was self-ligated to form pSPK11. As a result, two DNA fragments, *fadB'* and *fadA'*, corresponding to a partial 5' sequence of *fadB* and partial 3' sequence of *fadA* was inserted into pK18mobsacB in pSPK11. Plasmid pSPK09 or pSPK11 was first transformed into *E. coli* S17-1 by electroporation; transconjugation of *P. putida* strains and *E. coli* S17-1 harboring recombinant plasmids were carried out as described by Friedrich et al.<sup>25</sup>

**Mutation Procedure.** The method to generate a defined gene knockout mutant is described in Schäfer et al.<sup>26</sup> and our previous study.<sup>7</sup>

**Shake-Flask Culture Conditions.** Seed culture medium was LB medium containing (g L<sup>-1</sup>): yeast extract 5, Tryptone 10, and NaCl 10.

Mineral medium (MM) for one-step shake-flask cultivation contained the following (g L<sup>-1</sup>): fatty acids (sodium octanoate, decanoate, or dodecanoate) 12, (NH<sub>4</sub>)<sub>2</sub>SO<sub>4</sub> 1, MgSO<sub>4</sub>·7H<sub>2</sub>O 0.5, Na<sub>2</sub>HPO<sub>4</sub>·12H<sub>2</sub>O 9.65, KH<sub>2</sub>PO<sub>4</sub> 1.5, yeast extract 1, Fe(III)-NH<sub>4</sub>-citrate 0.05, CaCl<sub>2</sub> 0.02 and 1 mL L<sup>-1</sup> trace element solution. Trace element solution consisted of the following (mg L<sup>-1</sup>): ZnSO<sub>4</sub>·7H<sub>2</sub>O 100, MnCl<sub>2</sub>·4H<sub>2</sub>O 30, H<sub>3</sub>-BO<sub>3</sub> 300, CoCl<sub>2</sub>·6H<sub>2</sub>O 200, CuSO<sub>4</sub>·5H<sub>2</sub>O 10, NiCl<sub>2</sub>·6H<sub>2</sub>O 20, NaMoO<sub>4</sub>·2H<sub>2</sub>O 30, HCl 0.5 mol L<sup>-1</sup>.

Two-step shake-flask cultivation was conducted in LB medium for the first 9 h, and then fatty acids (sodium octanoate, decanoate, or dodecanoate) were added into the broth to a final concentration of 12 g L<sup>-1</sup>. The total culture time was 48 h.

The seed cultures were incubated at 30 °C in LB medium for 12 h at 200 rpm on a rotary shaker (NBS Series 25D, New Brunswick, U.S.A.) and were inoculated into shake-flask cultivation medium by a volume of 5%. Shake-flask cultivation was carried out at 30 °C for 48 h at 200 rpm on a rotary shaker (NBS Series 25D, New Brunswick, U.S.A.).

**Fermentor Culture Conditions.** A total of 15 mL of seed culture was prepared as described above and then inoculated into 300 mL of LB medium for 12 h cultivation under the same culture conditions. Subsequently, 300 mL of cultures served as an inoculant for the 6 L fermentor (NBS 3000, New Brunswick, U.S.A.) with a working volume of 3 L. The cells were grown at 30 °C and pH 6.3 (for one-step culture) or 7.0 (for two-step culture). Dissolved oxygen (DO) was provided by injecting filtered air at a flow rate of 0.5 L of filtered air per 1 L of culture broth per minute and was maintained at 20% of air saturation by automatically adjusting the agitation rate from 200 to 800 rpm. The pH was controlled automatically by addition of an aqueous solution of 5 M NaOH and 3 M H<sub>2</sub>SO<sub>4</sub>. Nitrogen limitation was not used in this study.

The initial culture medium for one-step culture in the fermentor contained the following (g L<sup>-1</sup>): dodecanoate 10, yeast extract 1, (NH<sub>4</sub>)<sub>2</sub>SO<sub>4</sub> 4.0, MgSO<sub>4</sub> 1.0, Na<sub>2</sub>HPO<sub>4</sub>·12H<sub>2</sub>O 4.5, KH<sub>2</sub>PO<sub>4</sub> 1.5, Fe-(III)-NH<sub>4</sub>-citrate 0.05, CaCl<sub>2</sub> 0.02 and 1 mL L<sup>-1</sup> trace element solution. A total of 30 g of dodecanoate was added into the fermentor when dodecanoate was exhausted.

The initial culture medium for two-step culture in the fermentor was LB media supplemented with 30 g L<sup>-1</sup> glucose. A total of 15 g of dodecanoate was added at 12 h, and 15 g of dodecanoate, 6 g of yeast extract, and 3 g of tryptone were added every 6 h when dodecanoate was exhausted.

**PHA Analysis, Extraction, and Purification.** The method for PHA analysis was the same as described previously.<sup>7</sup>

The extraction and purification of PHA was performed as described as previously.<sup>8</sup> Bacteria were harvested by centrifugation (8000 g, 10 min), subsequently washed with ethanol and distilled water, and then lyophilized. A total of 60 mL of acetyl butyrate was added into 10 g of dry cells and then treated at 75 °C for 1.5 h. Supernatant was obtained by centrifugation (8000 g, 10 min), and PHA was precipitated with 10 fold volume quantity of ethanol. The precipitated PHA was washed by ethanol and vacuum-dried. This method is safer than hot chloroform method, and the quality of PHA extracted by this method was the same.<sup>8</sup>

**Characterization of Physical Properties of PHA.** The molecular mass data for polyesters were obtained by GPC at 40 °C using a Spectra System P2000 equipped with Shimadzu HSG 60 column. Chloroform was used as eluent at a flow rate of 1 mL min<sup>-1</sup>, and sample

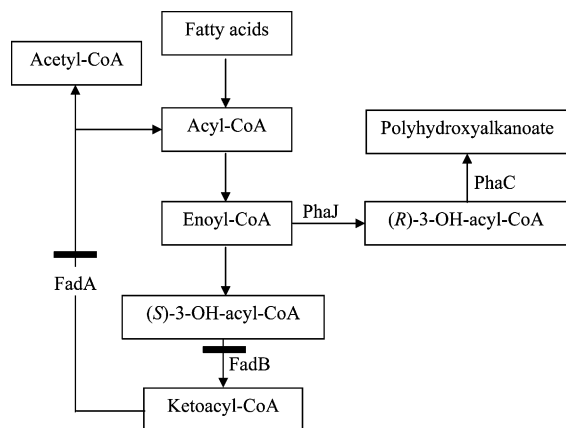


**Figure 1.** Deletion of  $\beta$ -oxidation pathway containing *fadB* and *fadA* genes in *Pseudomonas putida* KT2442,  $\beta$ -oxidation in mutant *P. putida* KTOY06 (derived from wild type KT2442) was weakened by deleting *fadB* and *fadA* genes. FadB: 3-hydroxyacyl-CoA dehydrogenase; FadA: 3-ketoacyl-CoA thiolase; PhaJ: (R)-specific Enoyl-CoA hydratase; PhaC: Polyhydroxyalkanoate synthase.

concentrations of 1 mg mL<sup>-1</sup> were applied. Polystyrene standards with low polydispersity were used to construct a calibration curve.

DSC was performed with a TA-Q100 DSC analyzer equipped with a mechanical cooler system. It was calibrated with an indium standard. Each sample weighting 2–3 mg was encapsulated in an aluminum pan and was heated from –80 to +100 °C as the first scan. After maintaining at 100 °C for 1 min, the molten sample was quenched to –80 °C. Subsequently, the sample was again heated from –80 to +100 °C as the second scan. A heating rate of 10 °C min<sup>-1</sup> was used throughout the process. Melting temperature ( $T_m$ ) and apparent heat of fusion ( $\Delta H_m$ ) were determined from the DSC endothermal peak value and areas of the first scan. Cold crystallization temperature ( $T_{cc}$ ) and heat of cold crystallization ( $\Delta H_{cc}$ ) were determined from the DSC exothermal peak value and areas in the second scan. The glass transition temperature ( $T_g$ ) was taken as the inflection point of the specific heat increment at the glass–rubber transition.

FTIR spectroscopy was used to determine the changes of crystallinity of PHA. Study was carried out with a Nicolet IR 200 (Thermo Electron Corporation, U.S.A.) spectroscope. A total of 32 scans at a resolution of 4 cm<sup>-1</sup> were recorded for each sample. Thin films of copolymers were cast from 10 mg mL<sup>-1</sup> solution in CHCl<sub>3</sub> on a KBr plate. All of the films were dried at room temperature. Complete removal of chloroform was confirmed by FTIR.

Tensile mechanical analysis was conducted on the PHA solvent-casting films. The films were cut into dumbbell-shape specimen with a width of 4 mm and a thickness of about 100  $\mu$ m. The stress–strain measurements of films were carried out using a CMT-4000 universal testing machine (Shenzhen SANS Corporation, China) at room temperature. Speed of the cross-head was 5 mm min<sup>-1</sup>.

## Results and Discussions

**Construction of *fadBA* Knockout Mutant of *P. putida* KT2442.** FadA and FadB catalyze the last two steps in  $\beta$ -oxidation pathway in *P. putida* KT2442 (Figure 1). Fatty acids entering into the  $\beta$ -oxidation pathway in the CoA form lose two carbon atoms in each cycle. For more MCL polyhydroxyalkanoate production, carbon flux could be directed more into PHA synthesis via weakening the  $\beta$ -oxidation pathway.

There were at least two sets of genes encoding putative proteins which were supposed to have catalysis abilities of 3-ketoacyl-CoA thiolase (FadAx or FadA) and 3-hydroxyacyl-CoA dehydrogenase (FadB2x or FadB) in *P. putida* KT2442's genome according to the data available in NCBI. *fadB2x* and *fadAx* (Locus tag PP\_2214 and PP\_2215) were two adjacent

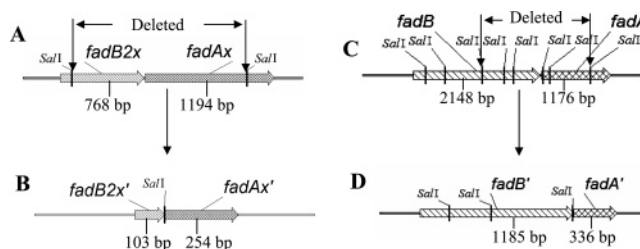


**Figure 2.** Details of chromosome DNA sequences in *Pseudomonas putida* KT2442 and its knockout mutants, (A) *fadB2x* and *fadAx* genes in *P. putida* KT2442; (B) *fadB2x* and *fadAx* genes were inactivated by deleting DNA fragment between two *SalI* sites as the arrow indicated in A; (C) *fadB* and *fadA* genes in *P. putida* KT2442; (D) *fadB* and *fadA* genes were inactivated by deleting DNA fragment between two *SalI* sites as the arrow indicated in C.

genes (Figure 2A), located in the middle of the *fad* operon in which *fadDx* and *fadB1x* were the upstream and downstream genes. *fadB* and *fadA* (Locus tag PP\_2136 and PP\_2137) (Figure 2C) formed an operon. The search on the *P. putida* KT2442 genome also indicated there were many putative proteins with similar functions. It was very difficult to delete all possible genes related to  $\beta$ -oxidation. In this study, only *fadB2x*, *fadAx*, *fadB*, and *fadA* were chosen as the target genes to investigate the relationship between  $\beta$ -oxidation and PHA synthesis.

The knockout of *fadB2x* and *fadAx* in *P. putida* KT2442 (Figure 2, panels A and B) using suicide plasmid pSPK09 led to the mutant termed *P. putida* KTOY04. Over 85% and 75% sequence of *fadB2x* and *fadAx*, respectively, was deleted in mutant KTOY04. Similarly, *fadB* and *fadA* knockout mutant of *P. putida* KT2442 using suicide plasmid pSPK11 formed *P. putida* KTOY06 and 50% sequence of *fadB*, and 70% sequence of *fadA* were deleted, respectively (Figure 2, panels C and D). To construct a double mutation on *P. putida* KTOY08, plasmid pSPK09 was used as the suicide plasmid and *P. putida* KTOY06 was used as the host. KTOY08 was a double mutant in which *fadB2x*, *fadB*, *fadAx*, and *fadA* lost their functions via deleting the same sequence as that in KTOY04 and KTOY06.

*P. putida* KT2442, KTOY04, KTOY06, and KTOY08 were cultured in mineral media using 12 g/L dodecanoate as the carbon source. Cell growth and PHA accumulation in *P. putida* KT2442 and KTOY04 was almost the same (Table 2), indicating that *fadB2x* and *fadAx* genes did not play a key role in the  $\beta$ -oxidation pathway. The *fadB fadA* knockout mutant *P. putida* KTOY06 grew to a cell dry weight (CDW) of only 2.17 g L<sup>-1</sup> containing 69% PHA. It was obvious that *fadB fadA* knockout mutant grew slower than the parent strain did but the mutant accumulated more PHA. It was very interesting to observe that PHA monomer compositions produced by *P. putida* KTOY06 was completely different from that of its parent strain. HDD fraction in PHA was increased from 7.5 mol % in the wild type to 35.7 mol % in the mutant. The *fadB2x fadAx fadB fadA* knockout mutant *P. putida* KTOY08 grew slower than *P. putida* KTOY06, which meant when *fadB fadA* did not exist the role of *fadB2x fadAx* became more important.

Yet PHA produced by *P. putida* KTOY06 still contained monomers with less than 12 carbon atoms, indicating  $\beta$ -oxidation was not completely blocked when only *fadB* and *fadA* genes were deleted. Otherwise, homogeneous PHA with only HDD monomer should be produced. However, it could be concluded that  $\beta$ -oxidation was significantly weakened. As a result, more carbon flux flowed to PHA accumulation rather than to cell growth. Thus, PHA produced by KTOY06 was found to contain more long chain length monomers than that by KT2442 (Table



**Table 2.** One-Step Culture of *P. putida* KT2442, KTOY04, KTOY06, and KTOY08 Using 12 g/L Dodecanoate as the Carbon Sources<sup>a</sup>

strain	CDW (g L <sup>-1</sup> )	PHA content (wt %)	PHA monomer composition (mol %)			
			HHx	HO	HD	HDD
KT2442	6.96 ± 0.28	50.5 ± 3.2	14.9 ± 0.4	51.6 ± 0.6	26.0 ± 0.4	7.5 ± 0.2
KTOY04	5.80 ± 0.35	56.7 ± 3.0	14.2 ± 0.2	51.9 ± 0.5	26.5 ± 0.4	7.4 ± 0.2
KTOY06	2.17 ± 0.14	69.9 ± 1.6	4.4 ± 0.2	31.9 ± 0.3	28.0 ± 0.7	35.7 ± 0.4
KTOY08	1.56 ± 0.19	19.8 ± 1.3	4.7 ± 0.9	34.6 ± 1.5	32.4 ± 1.8	28.3 ± 2.6

<sup>a</sup> Bacteria were cultured in mineral medium as described in the Material and Methods section at 30 °C for 48 h. All data were expressed as average value ± SD and represented the average value of three parallel experiments. CDW: cell dry weight; HHx: 3-hydroxyhexanoate; HO: 3-hydroxyoctanoate; HD: 3-hydroxydecanoate; HDD: 3-hydroxydodecanoate.

**Table 3.** Growth and MCL PHA Production by *P. putida* KT2442 and *P. putida* KTOY06 from Different Fatty Acids Using the One-Step Culture Process<sup>a</sup>

strain (carbon source)	CDW (g L <sup>-1</sup> )	PHA content (wt %)	PHA monomer composition (mol %)			
			HHx	HO	HD	HDD
KT2442 (C8)	5.35 ± 0.11	51.9 ± 0.6	18.8 ± 0.1	81.2 ± 0.8	0	0
KT2442 (C10)	3.37 ± 0.57	38.0 ± 3.4	16.6 ± 0.1	54.9 ± 0.4	28.5 ± 0.5	0
KT2442 (C12)	6.96 ± 0.28	50.5 ± 3.2	14.9 ± 0.4	51.6 ± 0.6	26.0 ± 0.4	7.5 ± 0.2
KTOY06 (C8)	0.59 ± 0.05	6.8 ± 0.9	5.5 ± 0.3	94.5 ± 0.3	0	0
KTOY06 (C10)	1.36 ± 0.31	35.8 ± 4.2	5.4 ± 0.2	52.5 ± 0.1	42.1 ± 0.1	0
KTOY06 (C12)	2.17 ± 0.14	69.9 ± 1.6	4.4 ± 0.2	31.9 ± 0.3	28.0 ± 0.7	35.7 ± 0.4

<sup>a</sup> Bacteria were cultured in mineral medium as described in the Material and Methods section at 30 °C for 48 h. All data were expressed as average value ± SD and represented the average value of three parallel experiments. C8: sodium octanoate; C10: decanoic acid; C12: dodecanoic acid; CDW: cell dry weight; HHx: 3-hydroxyhexanoate; HO: 3-hydroxyoctanoate; HD: 3-hydroxydecanoate; HDD: 3-hydroxydodecanoate.

**Table 4.** Growth and MCL PHA Production by *P. putida* KT2442 and *P. putida* KTOY06 from Different Fatty Acids Using the Two-Step Culture Process<sup>a</sup>

strain (carbon source)	CDW (g L <sup>-1</sup> )	PHA content (wt %)	PHA monomer composition (mol %)			
			HHx	HO	HD	HDD
KT2442 (C8)	6.42 ± 0.24	19.3 ± 1.2	20.6 ± 0.8	79.4 ± 0.8	0	0
KT2442 (C10)	3.79 ± 0.40	15.6 ± 1.3	16.5 ± 0.3	53.9 ± 0.2	29.7 ± 0.4	0
KT2442 (C12)	3.6 ± 0.28	43.7 ± 3.4	12.9 ± 0.5	39.1 ± 1.4	39.5 ± 2.3	8.5 ± 0.5
KTOY06 (C8)	1.76 ± 0.05	5.3 ± 0.7	7.2 ± 0.6	92.8 ± 0.6	0	0
KTOY06 (C10)	8.84 ± 0.32	76.1 ± 5.6	5.0 ± 0.2	47.2 ± 0.4	47.8 ± 0.5	0
KTOY06 (C12)	5.31 ± 0.24	84.3 ± 4.6	3.0 ± 0.1	22.9 ± 0.3	33.2 ± 1.0	40.9 ± 1.4

<sup>a</sup> Bacteria were cultured in LB media for 9 h at 30 °C, followed by fatty acids addition to the broth at a final concentration of 12 g/L. The total culture time was 48 h. All data were expressed as average value ± SD and represented the average value of three parallel experiments. C8: sodium octanoate; C10: decanoic acid; C12: dodecanoic acid; CDW: cell dry weight; HHx: 3-hydroxyhexanoate; HO: 3-hydroxyoctanoate; HD: 3-hydroxydecanoate; HDD: 3-hydroxydodecanoate.

2). These result indicated that *fadB* and *fadA* played an important role in  $\beta$ -oxidation pathway of *P. putida* KT2442.

**Production of PHA in *P. putida* KT2442 and its *fadB* and *fadA* Knockout Mutant KTOY06.** To compare cell growth and PHA accumulation by *P. putida* KTOY06 and its parent strain, different fatty acids were used as the carbon sources. When one-step culture was used (Table 3), growth of KTOY06 was slower than KT2442. It was clearly observed that mutant KTOY06 produced more longer chain length monomers in PHA compared with wild type KT2442. PHA produced by KTOY06 grown in dodecanoate contained 35.7 mol % HDD monomer compared with only 7.5 mol % HDD fraction in strain KT2442. When decanoate was used as the carbon source, mutant KTOY06 produced PHA containing 42.1 mol % HD, which was also much higher than that of 28.5 mol % HD produced by KT2442 (Table 3). In all cases, HHx fraction in PHA produced by mutant KTOY06 was much lower than its parent strain. All of these results demonstrated deletion of *fadB* and *fadA* genes weakened  $\beta$ -oxidation. As a result, cell growth and PHA accumulation was completely changed.

To increase cell growth and PHA accumulation, a two-step culture process was employed. Cell growth and PHA accumulation in KTOY06 grown in decanoate or dodecanoate was better than that in parent strain KT2442 (Table 4). However, cell

growth or PHA production was reduced when octanoate was used as a carbon source, so this could be attributed to the toxicity of octanoate especially when  $\beta$ -oxidation was weakened. Compared with the one-step process, the two-step approach provides extra nutrition for cell growth. Therefore, mutant KTOY06 produced more PHA containing more HDD monomer compared with that accumulated using the one-step process. In comparison, wild type KT2442 produced less PHA in the two-step process compared with the one step approach (Tables 3 and 4).

When grown on dodecanoate in the two-step process, *P. putida* KT2442 produced MCL PHA containing a large proportion of HO or HD monomer, with HDD fraction accounting for less than 10 mol % (Table 4). In comparison, the mutant KTOY06 accumulated over 40 mol % HDD as its PHA major fraction. At the same time, the mutant grew to 5.5 g L<sup>-1</sup> CDW containing 84 wt % MCL PHA with very high HDD fraction after a 48 h shake-flask cultivation. For the very first time, a new type of MCL PHA containing high HDD fraction was obtained.

**Production of MCL PHA by *P. putida* KTOY06 in a 6-L Fermentor.** The *fadB* and *fadA* knockout mutant *P. putida* KTOY06 was grown in a 6-L fermentor to investigate dynamic cell growth and PHA accumulation during the cultivation

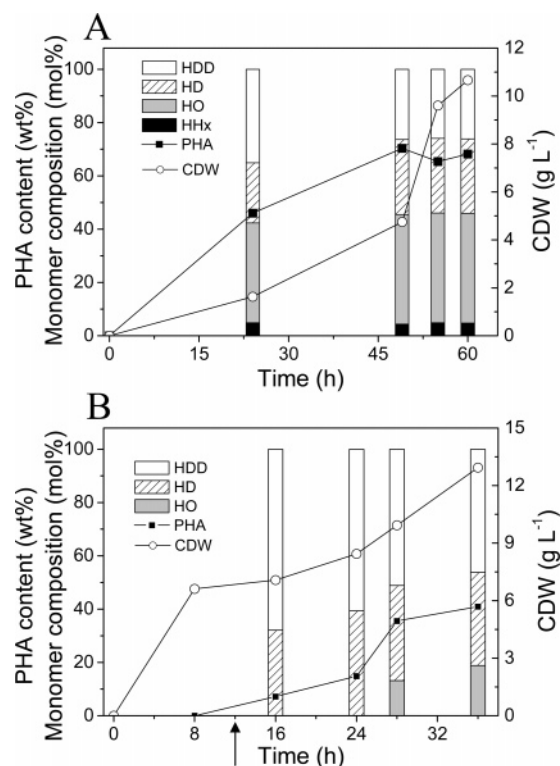


**Figure 3.** Cell growth, PHA production, and monomer composition produced by *Pseudomonas putida* KTOY06 grown in a 6-L fermentor. (A) The one-step growth process. Strains were grown on dodecanoate as the carbon source; (B) The two-step growth process. Strains were grown on LB medium supplemented with glucose for the first stage, and then dodecanoate, yeast and tryptone were added for the second stage culture at 12 h as the arrow indicated.

process. When the one-step culture process was used, cell growth on dodecanoate was very slow (Figure 3A): the lag phase lasted over 24 h. Exponential growth occurred during 48–60 h. PHA content increased slowly from 46 wt % at 24 h to nearly 70 wt % at 48 h and remained stable afterward. HDD fraction in PHA decreased slowly from 35 to 26 mol % during the growth process. At the end of the culture at 60 h, 10.7 g L<sup>-1</sup> CDW containing 68.2 wt % PHA was produced, in which HHx, HO, HD, and HDD fractions were 4.8, 41.2, 28.0, and 26.1 mol %, respectively. In comparison, wild type *P. putida* KT2442 cultured under the same conditions in the 6-L fermentor produced PHA consisting of 9.5 mol % HHx, 42.6 mol % HO, 32.9 mol % HD, and 15.0 mol % HDD (data not shown), very similar to the results obtained from shake-flask culture (Table 3).

In the two-step culture process, yeast extract, tryptone, and glucose served as nutrition to support cell growth, less than 0.1 wt % PHA was produced before dodecanoate was added at 12 h (Figure 3B). Interestingly, no HHx monomer was detected during the whole culture process. No HO monomer was observable at the first several hours when dodecanoate was added. The HO monomer started to be incorporated into the polymer during the 24–28 h growth period. The PHA monomer composition dynamically changed during 16–36 h, with the HO fraction increasing from 0 to 19 mol %, the HD fraction slightly increasing from 32 to 35 mol %, and the HDD fraction decreasing from 68 mol % at 16 h to 46 mol %. At the end of the culture at 36 h, 12.9 g L<sup>-1</sup> CDW containing 41.0 wt % PHA was obtained.

Dodecanoate provides monomers for PHA synthesis, and it could also support bacterial growth. When the  $\beta$ -oxidation

pathway was weakened, more dodecanoate metabolites flowed to the PHA production pathway. That was why the HDD fraction was increased dramatically in the *P. putida* KTOY06 mutant defective in  $\beta$ -oxidation compared with the parent strain KT2442. However, the  $\beta$ -oxidation pathway was not completely blocked. Thus, carbon flux might flow into cell growth especially when fatty acids were used as the sole carbon sources. Therefore, the PHA monomer composition produced by KTOY06 depended on the growth condition. With high survival pressure to use fatty acids to support bacterial growth, for instance, under the growth condition of the one-step culture, the HDD fraction was lower. When extra carbon sources were available to support bacterial growth, fatty acids were mainly used for PHA accumulation. In this case, for instance, when the two-step process was used, the HDD fraction in PHA was much higher. This growth-condition-dependent phenomenon could not be observed in wild type *P. putida* KT2442. The monomer composition of PHA produced by KT2442 was relatively stable under all culture conditions (Tables 3 and 4).

**Physical Properties of MCL PHA with Different HDD Fractions.** MCL PHA with different HDD fractions (15, 28, or 39 mol %) were prepared by using *P. putida* KT2442 or KTOY06 as the host. Weight-average molecular weights ( $M_w$ ), number-average molecular weights ( $M_n$ ), and polydispersity ( $M_w/M_n$ ) of PHA accumulated in *P. putida* KTOY06 were similar with that accumulated in *P. putida* KT2442 (Table 5).

Thermal properties of PHA with different HDD fraction were determined. (Figure 4, Table 5). When the HDD fraction in the MCL PHA increased from 15 to 39 mol %,  $T_m$  increased from 53 to 65 °C and  $\Delta H_m$  increased from 18 to 28 J g<sup>-1</sup>, respectively (Table 5). This may reflect that a higher HDD fraction favored MCL PHA to crystallize. These results were in good agreement with what Gross et al.<sup>27</sup> and Preusting et al.<sup>28</sup> studied. They found that a higher endotherm suggests a higher degree of sample crystallinity. By comparing with MCL PHA in this study, some MCL PHA derived from hexanoate, octanoate, or dodecanoate carbon sources have much lower  $T_m$  and  $\Delta H_m$  as reported.<sup>27–29</sup>  $T_g$  remained relatively constant with the variation of HDD fraction. When the HDD fraction reached 39 mol % (curve c in Figure 4A), MCL PHA had the highest  $\Delta H_{cc}$ , and three cold crystallization peaks located at -13, 21, and 34 °C, respectively, were observed. As it was detected, the HDD fraction in MCL PHA produced by *P. putida* KTOY06 decreased over time during the fermentation process, and different cold crystallization peaks may reflect the difference of crystallization ability of MCL PHA with the variation of HDD fraction.

A nonisothermal crystallization procedure at a cooling rate of 5 °C min<sup>-1</sup> was carried out. MCL PHA with 39 mol % HDD units had the highest peak crystallization temperature ( $T_c$ ) at 27 °C and highest crystallization enthalpy ( $\Delta H_c$ ) valued for 26 J g<sup>-1</sup>, whereas that for MCL PHA with 15 mol % HDD units were hardly observed (curve a in Figure 4B). Generally, a higher  $T_c$  and higher  $\Delta H_c$  indicated faster crystallization and better crystallizability of a polymer.<sup>30</sup>

FTIR was sensitive to the local molecular environment of polymers and therefore was found as a sensitive probe for the crystallinity degree of PHA.<sup>31–32</sup> The changes of crystallinity was confirmed by FTIR (Figure 5, panels a and b). The bands at 1170 and 1743 cm<sup>-1</sup> are characteristic of the amorphous phase in MCL PHA and that at 1728 cm<sup>-1</sup> is characteristic of the crystalline phase. The bands at 1728 and 1743 cm<sup>-1</sup> (Figure 5a) are assigned to the stretching vibrations of the crystalline and amorphous carbonyl (C=O) groups of MCL PHA, respec-

**Table 5.** Physical Properties of MCL PHA with Different HDD Fractions

strain (carbon source)	HDD fraction (mol %)	molecular weights <sup>d</sup>			thermal properties <sup>e</sup>						mechanical properties <sup>g</sup>			
		$M_w$ , $\times 10^4$ Da	$M_n$ , $\times 10^4$ Da	$M_w/M_n$	$T_m$ , °C	$\Delta H_m$ , J g <sup>-1</sup>	$T_{cc}$ , °C	$\Delta H_{cc}$ , J g <sup>-1</sup>	$T_g$ , °C	CI <sup>f</sup>	$E$ , MPa	$\epsilon_t$ , MPa	$\sigma_b$ , MPa	$\epsilon_b$ , %
KT2442 (C12) <sup>a</sup>	15	10.0	8.0	1.25	53	18	28	7	-44	0.23	3.6	8.7	5.0	188.7
KTOY06 (C12) <sup>b</sup>	28	13.4	9.5	1.41	58	22	-7	8	-45	0.32	6.0	12.6	6.5	180.0
KTOY06 (C12) <sup>c</sup>	39	15.7	10.8	1.45	65	28	-15	16	-43	0.46	11.5	16.3	8.9	125.0
							21	2						
							34	16						

<sup>a</sup> One-step culture of *P. putida* KT2442 in a 6-L fermentor. <sup>b</sup> One-step culture of *P. putida* KTOY06 in a 6-L fermentor. <sup>c</sup> Two-step culture of *P. putida* KTOY06 in a shake flask. <sup>d</sup> Molecular weights determined by GPC.  $M_w$ , weight-average molecular weight;  $M_n$ , number-average molecular weight;  $M_w/M_n$ , polydispersity. <sup>e</sup> DSC Thermal properties:  $T_m$ , melting temperature;  $\Delta H_m$ , apparent heat of fusion;  $T_{cc}$ , cold crystallization temperature;  $\Delta H_{cc}$ , heat of cold crystallization;  $T_g$ , glass transition temperature. <sup>f</sup> Crystallinity index (CI) defined as the ratio of the intensities of the FTIR bands at 1381 cm<sup>-1</sup> to the band at 1170 cm<sup>-1</sup>. <sup>g</sup>  $E$ , Young's modulus;  $\epsilon_t$ , tensile strength;  $\sigma_b$ , stress at break;  $\epsilon_b$ , elongation at break.

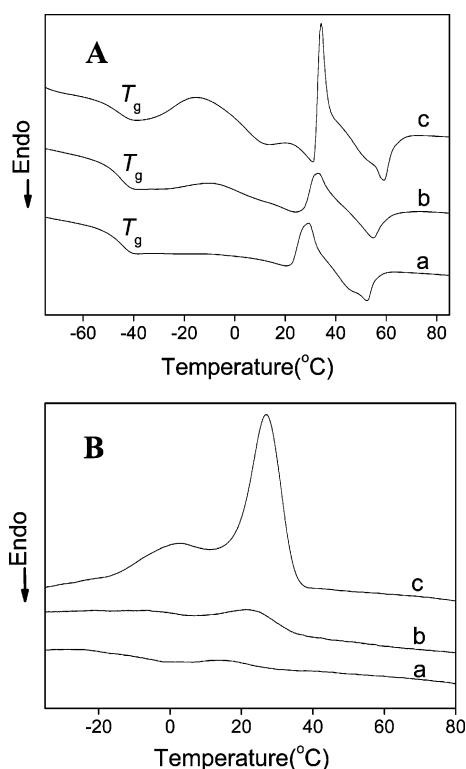


**Figure 4.** (A) DSC thermograms (second run) of MCL PHA with different HDD fraction. (B) DSC thermograms recorded by cooling the sample from +100 to -80 °C at a cooling rate of 5 °C min<sup>-1</sup>. (a) MCL PHA with 15 mol % HDD. (b) MCL PHA with 28 mol % HDD. (c) MCL PHA with 39 mol % HDD.  $T_g$ : glass-transition temperature.

tively. When the HDD fraction was 15 mol %, the spectral intensity at 1728 cm<sup>-1</sup> corresponding to the crystalline phase of MCL PHA was hardly observed, whereas that for MCL PHA with 39 mol % HDD appeared obviously. For an overall view, the band shapes in the wavelength region of 1600–1900 cm<sup>-1</sup> became broader with decreasing contents of HDD fraction. This demonstrates the existence of more molecular freedom in MCL PHA with decreasing contents of HDD fraction. As demonstrated by Bloembergen et al.,<sup>32</sup> the intensity of the band at 1381 cm<sup>-1</sup> is insensitive to the crystallinity and copolymer composition of PHA, whereas that at 1170 cm<sup>-1</sup> has the largest difference between the crystalline and amorphous states. Therefore, a crystallinity index (CI) was defined as the ratio of the intensities of the bands at 1381 cm<sup>-1</sup> to the band at 1170 cm<sup>-1</sup> to quantitatively measure the crystallinity degree of MCL PHA (Figure 5b). When the HDD fraction increased from 15

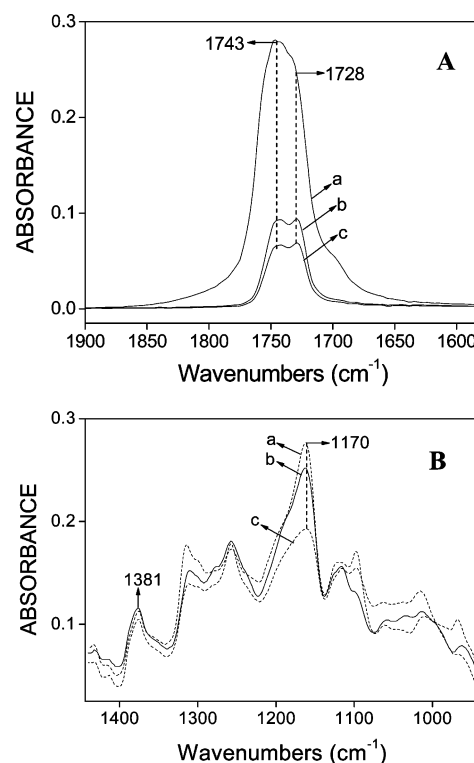


**Figure 5.** FTIR spectra of MCL PHA. (A) Variance of the C=O stretching band of MCL PHA with different HDD fraction. (a) MCL PHA with 15 mol % HDD. (b) MCL PHA with 28 mol % HDD. (c) MCL PHA with 39 mol % HDD. (B) Comparison of amorphous-phase sensitive peak (1170 cm<sup>-1</sup>) of solution-cast MCL PHA samples containing different HDD fractions. (a) MCL PHA with 15 mol % HDD. (b) MCL PHA with 28 mol % HDD. (c) MCL PHA with 39 mol % HDD.

to 39 mol %, the CI value increased from 0.23 to 0.46, reflecting a higher crystallinity.

Stress-strain curves of MCL PHA with different HDD fraction were recorded (Figure 6). Related parameters of Young's modulus ( $E$ ), tensile strength ( $\epsilon_t$ ), stress at break ( $\sigma_b$ ), and elongation at break ( $\epsilon_b$ ) were compared (Table 5). All of the MCL PHA samples showed some behaviors of thermoplastic elastomers. No yield points were observed for all of the MCL PHA. These MCL PHA samples combined both good tensile strength and desirable elongation at break, which make them far more superior than PHB and PHBV in terms of requirement for applications. When the HDD fraction was increased, the  $E$ ,  $\epsilon_t$ , and  $\sigma_b$  increased from 3.6, 8.7, and 5.0 MPa to 11.5, 16.3, and 8.9 MPa, respectively, whereas  $\epsilon_b$  decreased from 188.7% to 125.0%. Unlike the reported MCL PHA which have higher  $\epsilon_b$  of 300–500%,<sup>29</sup> MCL PHA in this study show intermediate



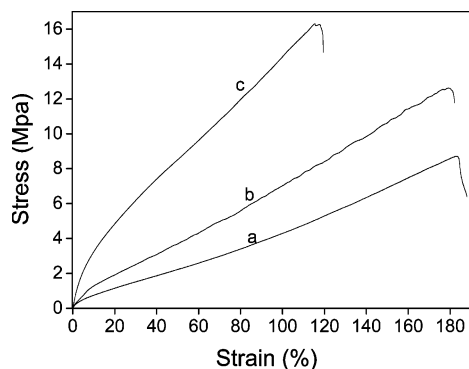


**Figure 6.** Stress–strain curves for MCL PHA with different HDD fractions. (a) MCL PHA with 15 mol % HDD. (b) MCL PHA with 28 mol % HDD. (c) MCL PHA with 39 mol % HDD.

$\epsilon_b$ . This may be correlated with the changes of crystallization with the variation of HDD fractions. Generally, higher crystallization will result in a more brittle polymer which is characterized by higher  $E$ ,  $\epsilon_t$ , and  $\sigma_b$  and lower  $\epsilon_b$ .

### Conclusions

A convenient gene knockout method was developed for *Pseudomonas putida* KT2442. Mutant *P. putida* KTOY04 (*fadB2x* and *fadAx* knockout mutant), KTOY06 (*fadB* and *fadA* knockout mutant), and KTOY08 (*fadB2x*, *fadAx*, *fadB*, and *fadA* knockout mutant) were used to investigate the effect of impaired  $\beta$ -oxidation on PHA accumulation. The result showed that *fadB* and *fadA* played a more important role in fatty acid degradation than other putative genes. However, the deletion of *fadB fadA* could not completely block the  $\beta$ -oxidation pathway.

PHA accumulation in the  $\beta$ -oxidation pathway weakened mutant KTOY06 (*fadB* and *fadA* knockout mutant) contained more monomer fraction with long carbon length. When dodecanoate was used as the carbon source, the HDD fraction in PHA produced by *P. putida* KTOY06 was 25–41 mol %, depending on the culture scale and growth conditions, which was much higher than that of 7–15 mol % produced by its parent strain KT2442. PHA with a high HDD fraction was obtained for the first time.

By comparing MCL PHA with different HDD fractions, for the first time, it was found that a higher HDD fraction will provide MCL PHA with a higher crystallization degree and tensile strength. These properties are required for many applications.

**Acknowledgment.** We are very grateful for the kind donation of plasmid pK18mobsacB from Dr. Andreas Schäfer of the University of Bielefeld (Bielefeld, Germany) and *Pseudomonas putida* KT2442 from Dr. Bernard Witholt (ETH Zürich, Switzerland). This study was financially supported by Hi-Tech Research and Development Program of China (863 Program; Grant Nos. 2006AA02Z242 and 2006AA020104). G.Q.C. was also supported by the National Basic Research Program of China (973 Program; Grant No. 2007CB707804). We are also very grateful for the Li Ka-Shing foundation which also provided support to G.Q.C. and R.C.L.

### References and Notes

- Anderson A. J.; Dawes E. A. Occurrence, metabolism, metabolic role, and industrial use of bacterial polyhydroxyalkanoates. *Microbiol. Rev.* **1990**, *54*, 450–472.
- Suriyamongkol, P.; Weselake, R.; Narine, S.; Moloney, M.; Shah, S. Biotechnological approaches for the production of polyhydroxyalkanoates in microorganisms and plants—A review. *Biotechnol. Adv.* **2007**, *25*, 148–175.
- Solaiman, D. K.; Ashby, R. D.; Foglia, T. A. Physiological characterization and genetic engineering of *Pseudomonas corrugata* for medium-chain-length polyhydroxyalkanoates synthesis from triacylglycerols. *Curr. Microbiol.* **2002**, *44*, 189–195.
- Hazer, B.; Steinbüchel, A. Increased diversification of polyhydroxyalkanoates by modification reactions for industrial and medical applications. *Appl. Microbiol. Biotechnol.* **2007**, *74*, 1–12.
- Chen, G. Q.; Wu, Q. The application of polyhydroxyalkanoates as tissue engineering materials. *Biomaterials* **2005**, *26*, 6565–6578.
- Zhao, K.; Deng, Y.; Chen, J. C.; Chen, G. Q. Polyhydroxyalkanoate (PHA) scaffolds with good mechanical properties and biocompatibility. *Biomaterials* **2003**, *24*, 1041–1045.
- Ouyang, S. P.; Liu, Q.; Fang, L.; Chen, G. Q. Construction of pha-Operon-Defined Knockout Mutants of *Pseudomonas putida* KT2442 and their applications in poly(hydroxyalkanoate) production. *Macromol. Biosci.* **2007**, *7*, 227–233.
- Chen, G. Q.; Ouyang, S. P. A novel method for the extraction of Polyhydroxyalkanoates from microorganisms. China Patent, CN1-844185.
- Ashby, R. D.; Foglia, T. A.; Solaiman, D. K.; Liu, C.; Nunez, A.; Eggink, G. Viscoelastic properties of linseed oil-based medium chain length poly(hydroxyalkanoate) films: Effects of epoxidation and curing. *Int. J. Biol. Macromol.* **2000**, *28*, 355–361.
- Noda, I.; Satkowski, M. M.; Dowrey, A. E.; Marcott, C. Polymer alloys of Nodax copolymers and poly(lactic acid). *Macromol. Biosci.* **2004**, *4*, 269–275.
- Diniz, S. C.; Taciro, M. K.; Gomez, J. G.; da Cruz Pradella, J. G. High-cell-density cultivation of *Pseudomonas putida* IPT 046 and medium-chain-length polyhydroxyalkanoate production from sugarcane carbohydrates. *Appl. Biochem. Biotechnol.* **2004**, *Oct*, 119 (1), 51–70.
- Kroumova, A. B.; Wagner, G. J.; Davies, H. M. Biochemical observations on medium-chain-length polyhydroxyalkanoate biosynthesis and accumulation in *Pseudomonas mendocina*. *Arch. Biochem. Biophys.* **2002**, *405*, 95–103.
- Sánchez, R. J.; Schripsema, J.; da Silva, L. F.; Taciro, M. K.; Pradella, J. G. C.; Gomez, J. G. C. Medium-chain-length polyhydroxyalkanoic acids (PHAmcl) produced by *Pseudomonas putida* IPT 046 from renewable sources. *Eur. Polym. J.* **2003**, *39*, 1385–1394.
- Fiedler, S.; Steinbüchel, A.; Rehm, B. The role of the fatty acid  $\beta$ -oxidation multienzyme complex from *Pseudomonas oleovorans* in polyhydroxyalkanoate biosynthesis: molecular characterization of the *fadBA* operon from *P. oleovorans* and of the enoyl-CoA hydratase genes *phaJ* from *Pseudomonas oleovorans* and *Pseudomonas putida*. *Arch. Microbiol.* **2002**, *178*, 149–160.
- Snell, K. D.; Feng, F.; Zhong, L. H.; Martin, D.; Madison, L. L. YfcX enables medium-chain-length poly(3-hydroxyalkanoate) formation from fatty acids in recombinant *Escherichia coli fadB* Strains. *J. Bacteriol.* **2002**, *184*, 5696–5705.
- Park, S. J.; Lee, S. Y. New FadB homologous enzymes and their use in enhanced biosynthesis of medium-chain-length polyhydroxyalkanoates in *fadB* mutant *Escherichia coli*. *Biotechnol. Bioeng.* **2004**, *86*, 681–686.
- Park, S. J.; Lee, S. Y. Biosynthesis of poly(3-hydroxybutyrate-co-3-hydroxyalkanoates) by metabolically engineered *Escherichia coli* strains. *Appl. Biochem. Biotechnol.* **2004**, *113*, 335–346.
- Olivera, E. R.; Carnicero, D.; Jodra, R.; Minambres, B.; Garcia, B.; Abraham, G. A.; Gallardo, A.; San Roman, J.; Garcia, J. L.; Naharro, G.; Luengo, J. M. Genetically engineered *Pseudomonas*: A factory of new bioplastics with broad applications. *Environ. Microbiol.* **2001**, *3*, 612–618.
- Green, P. R.; Kemper, J.; Schechtman, L.; Guo, L.; Satkowski, M.; Fiedler, S.; Steinbüchel, A.; Rehm, B. H. A. Formation of short chain length/medium chain length polyhydroxyalkanoate copolymers by fatty acid  $\beta$ -oxidation inhibited *Ralstonia eutropha*. *Biomacromolecules* **2002**, *3*, 208–213.
- de Oliveira, V. C.; Maeda, I.; Delessert, S.; Poirier, Y. Increasing the carbon flux toward synthesis of the short-chain-length-medium-chain-length polyhydroxyalkanoate in the peroxisome of *Saccharomyces*

- cerevisiae* through modification of the beta-oxidation cycle. *Appl. Environ. Microbiol.* **2004**, *70*, 5685–5687.
- (21) Kellerhals, M. B.; Kessler, B.; Witholt, B. Closed-loop control of bacterial high-cell-density fed-batch cultures: Production of mcl-PHAs by *Pseudomonas putida* KT2442 under single-substrate and cofeeding conditions. *Biotechnol. Bioeng.* **1999**, *65*, 306–315.
  - (22) Sun, Z. Y.; Ramsay, J. A.; Guay, M.; Ramsay, B. A. Automated feeding strategies for high-cell-density fed-batch cultivation of *Pseudomonas putida* KT2440. *Appl. Microbiol. Biotechnol.* **2006**, *71*, 423–431.
  - (23) Sun, Z.; Ramsay, J. A.; Guay, M.; Ramsay, B. A. Carbon-limited fed-batch production of medium-chain-length polyhydroxyalkanoates from nonanoic acid by *Pseudomonas putida* KT2440. *Appl. Microbiol. Biotechnol.* **2007**, *74*, 69–77.
  - (24) Weinl, C.; Nelson, K. E.; Tummeler, B. Global features of the *Pseudomonas putida* KT2440 genome sequence. *Environ. Microbiol.* **2002**, *4*, 809–818.
  - (25) Friedrich, B.; Hogrefe, C.; Schlegel, H. G. Naturally occurring genetic transfer of hydrogen-oxidizing ability between strains of *Alcaligenes eutrophus*. *J. Bacteriol.* **1981**, *147*, 198–205.
  - (26) Schäfer, A.; Tauch, A.; Jäger, W.; Kalinowski, J.; Thierbach, G.; Pühler, A. Small mobilizable multi-purpose cloning vectors derived from the *Escherichia coli* plasmids pK18 and pK19: selection of defined deletions in the chromosome of *Corynebacterium glutamicum*. *Gene* **1994**, *145*, 69–73.
  - (27) Gross, R. A.; Demello, C.; Lenz, R. W.; Brandl, H.; Fuller, R. C. Biosynthesis and characterization of poly( $\beta$ -hydroxyalkanoates) produced by *Pseudomonas oleovorans*. *Macromolecules* **1989**, *22*, 1106–1115.
  - (28) Preusting, H.; Nijenhuis, A.; Witholt, B. Physical characterization of poly(3-hydroxyalkanoates) and poly(3-hydroxyalkenoates) produced by *Pseudomonas oleovorans* growth on aliphatic hydrocarbons. *Macromolecules* **1990**, *23*, 4220–4224.
  - (29) Gagnon, K. D.; Lenz, R. W.; Farris, R. J.; Fuller, R. Crystallization behavior and its influence on the mechanical properties of a thermoplastic elastomer produced by *Pseudomonas oleovorans*. *Macromolecules* **1992**, *25*, 3723–3728.
  - (30) Dong, T.; He, Y.; Zhu, B.; Shin, K. M.; Inoue, Y. Nucleation mechanism of  $\alpha$ -cyclodextrin-enhanced crystallization of some semicrystalline aliphatic polymers. *Macromolecules* **2005**, *38*, 7736–7744.
  - (31) Scandola, M.; Focarete, M. L.; Adamus, G.; Sikorska, W.; Baranowska, I.; Swierczek, S.; Gnatowski, M.; Kowalczyk, M.; Jedlinski, Z. Polymer blends of natural poly(3-hydroxybutyrate-co-3-hydroxyvalerate) and a synthetic atactic poly(3-hydroxybutyrate): Characterization and biodegradation studies. *Macromolecules* **1997**, *30*, 2568–2574.
  - (32) Bloembergen, S.; Holden, D. A.; Hamer, G. K.; Bluhm, T. L.; Marchessault, R. H. Study of composition and crystallization of bacterial poly( $\beta$ -hydroxybutyrate-co- $\beta$ -hydroxyvalerate). *Macromolecules* **1986**, *19*, 2865–2871.

BM0702307